Local field distributions in spin glasses

2008 J. Phys. A: Math. Theor. 41 324007

(http://iopscience.iop.org/1751-8121/41/32/324007)

IOP PUBLISHING JOURNAL OF PHYSICS A: MATHEMATICAL AND THEORETICAL

J. Phys. A: Math. Theor. **41** (2008) 324007 (15pp) doi:10.1088/1751-8113/41/32/324007

Local field distributions in spin glasses

Stefan Boettcher[1], **Helmut G Katzgraber**[2] **and David Sherrington**[3]

[1] Physics Department, Emory University, Atlanta, Georgia 30322, USA
[2] Theoretische Physik, ETH Zürich, CH-8093 Zürich, Switzerland
[3] Rudolf Peierls Centre for Theoretical Physics, University of Oxford, 1 Keble Road, Oxford, OX1 3NP, UK

E-mail: sboettc@emory.edu, katzgraber@phys.ethz.ch and d.sherrington1@physics.oxford.ac.uk

Received 25 November 2007, in final form 2 February 2008
Published 30 July 2008
Online at stacks.iop.org/JPhysA/41/324007

Abstract
Numerical results for the local field distributions of a family of Ising spin-glass models are presented. In particular, the Edwards–Anderson model in dimensions two, three and four is considered, as well as spin glasses with long-range power-law-modulated interactions that interpolate between a nearest-neighbour Edwards–Anderson system in one dimension and the infinite-range Sherrington–Kirkpatrick model. Remarkably, the local field distributions only depend weakly on the range of the interactions and the dimensionality, and show strong similarities except for near-zero local field.

PACS numbers: 75.50.Lk, 75.40.Mg, 05.50.+q

(Some figures in this article are in colour only in the electronic version)

1. Introduction

There has been interest in the distribution $P(h, T)$ of local fields h at temperature T in spin glasses since the earliest days of their theoretical study [1, 2]. Particularly influential was Thouless, Anderson and Palmer's [3] (TAP) self-consistent solution of $P(h, T = 0)$ for the Sherrington–Kirkpatrick [4] (SK) infinite-ranged spin-glass model for which a mean-field theory is believed to be exact, albeit unusual and very subtle [5, 6]. Since then there have been several further studies of $P(h)$ for the SK model (see, for example, [7–10]) and the nature of the local field distributions is well understood. On the other hand, there has been little work on the study of $P(h)$ for other spin-glass models. Most notably, few studies exist of $P(h)$ for the finite-range canonical Edwards–Anderson [11, 12] (EA) Ising spin-glass model which is generally not exactly solvable. It remains controversial whether some of the specific subtleties of the SK model are applicable to the EA model and other more realistic models, and their relationship is far from clear.

This paper studies and compares numerically the local field distributions at $T = 0$ of Ising spin glasses with varying range-behaviour and spatial dimensionality, which are largely inaccessible to exact solution. We focus our discussion to Gaussian bond distributions of zero mean. A remarkable and somewhat surprising similarity is found across systems for which other aspects of the statistical physics state structure are believed to be different, but with systematic small differences near $h = 0$ as the system interpolates between the limits of one-dimensional nearest-neighbour and infinite-ranged mean field, at both extremes of which $P(h = 0, T = 0)$ is zero in the thermodynamic limit.

The paper is structured as follows. In section 2, we introduce the models studied followed by brief descriptions of the numerical methods in section 3. Our results are presented in section 4 followed by concluding remarks.

2. Models

Both the SK model and the EA models are characterized by the Hamiltonian

$$\mathcal{H} = -\sum_{i<j} J_{ij} S_i S_j, \tag{1}$$

where $S_i \in \{\pm 1\}$. The interactions J_{ij} are chosen randomly and independently from a Gaussian distribution of zero mean and then quenched. In the SK model the sum over i and j extends over all sites and the variance of the distribution $\mathcal{P}(J_{ij})$ scales inversely with the system size N as J^2/N. Here we set $J = 1$ so that the spin-glass onset transition is at $T_c = 1$. For the EA model, the sum over the indices i and j is restricted to nearest-neighbour pairs and the variance of the bonds J_{ij} is independent of the number of spins N on a d-dimensional hyper-cubic lattice of size $N = L^d$; in this case, unlike for the SK model, the lattice dimension is relevant both qualitatively and quantitatively. There is universal agreement that the SK model exhibits a phase transition as the temperature is reduced [13] to a phase with an ultrametric hierarchy of metastable states and an associated mathematical feature of replica-symmetry breaking of the overlap order parameter. For the finite-range EA model there is a spin-glass transition above the lower critical dimension, $d > d_l$, believed [14] to be $d_l = 5/2$, but the existence of an ultrametric hierarchy in short-range systems is controversial, not proven and disbelieved by many practitioners.

In order to effectively interpolate between the physics of the SK and EA models and to probe their similarities and differences we also study a 'tunable' model first introduced by Kotliar, Anderson and Stein (KAS) [16] and recently studied in detail by Katzgraber and Young [17–20]. The model, which has helped elucidate many properties of spin glasses, is a long-range Ising spin glass with random power-law interactions. The Hamiltonian of the model is given by equation (1) but now with the sites i and j on a d-dimensional lattice with periodic boundary conditions and the exchange interactions given by

$$J_{ij} = c(\sigma)\frac{\epsilon_{ij}}{{r_{ij}}^{\sigma}}. \tag{2}$$

Here, r_{ij} is the separation of spins i and j, ϵ_{ij} are chosen randomly and independently from a Gaussian distribution of zero mean and standard deviation unity, and $c(\sigma)$ is a constant. The KAS model is believed to interpolate between mean-field-like behaviour for small $\sigma < \sigma_{c1}(d)$, an intermediate long-range regime $[\sigma_{c1}(d) < \sigma < \sigma_{c2}(d)\ ]$, and a short-range regime $[\sigma_{c2}(d) < \sigma < \sigma_{c3}(d) = \infty\ ]$. Each of the latter two regimes are subdivided into ordering and non-ordering regimes depending upon the space dimension (higher dimensions favouring ordering); see figure 1. In the present work, we shall consider only $d = 1$ for the KAS model, for which case the intermediate long-range region has a finite-cooperative-ordering

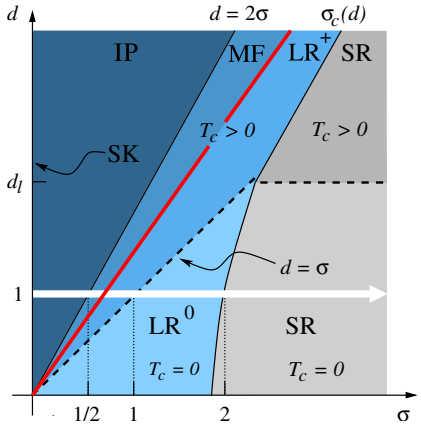

Figure 1. Schematic phase diagram of the KAS model in the d–σ plane following [15]. In this work, we focus on $d = 1$ which corresponds to the white horizontal arrow. For $\sigma \leqslant 1/2$ we expect infinite-range (IR) behaviour reminiscent of the SK model and where the energy needs to be rescaled as a power of the system size to avoid divergences, whereas for $1/2 < \sigma \leqslant 2/3$ we have mean-field (MF) behaviour corresponding to an effective space dimension $d_{\rm eff} \geqslant 6$ (the thickened line separates mean-field from non-mean-field behaviour). For $2/3 < \sigma \lesssim 1$ we have a long-range (LR^+) spin glass with a finite-ordering temperature $T_{\rm c}$, whereas for $1 \lesssim \sigma \lesssim 2$ we have a long-range spin glass with $T_{\rm c} = 0$ (LR^0). For $\sigma \gtrsim 2$ the model displays short-range (SR) behaviour with a zero transition temperature [16, 17]. Empirically, for $0.5 \leqslant \sigma \lesssim 1$ the $d = 1$ KAS model can be identified as corresponding to an EA system with effective dimension $d_{\rm eff} \approx 2/(2\sigma - 1)$ [13]. Figure adapted from [17].

temperature $T_{\rm c} > 0$ for $\sigma < \sigma_{\rm c}$ but no finite-temperature ordering for $\sigma > \sigma_{\rm c}$; see figure 1. To enforce periodic boundary conditions we place the spins on a ring (see [17] for details) and choose the geometric distance between the spins, i.e., $r_{ij} = (N/\pi)\sin(\pi|i-j|/N)$. We normalize the interactions to have $T_{\rm c}^{\rm MF} = 1$ for all σ, i.e.,

$$c(\sigma)^{-2} = \sum_{j \neq i} {r_{ij}}^{-2\sigma}. \tag{3}$$

For the short-range EA model we study hyper-cubic lattices in different space dimensions d. Again, in order to assist quantitative comparisons, in all cases we choose the exchange-scale normalization to yield the same mean-field transition temperature $T_{\rm c}^{\rm MF} = 1$. Hence for EA models we choose the variance of the exchange to be $1/z$ where z is the coordination number; for the hyper-cubic lattices that we study $z = 2d$. In the thermodynamic limit the SK model is equivalent to the infinite-dimensional EA model; hence, its normalization with the variance of the exchange interactions scaling as $1/N$.

3. Numerical procedures

For the EA model, we apply the extremal optimization (EO) heuristic as described in [21]. EO provides approximate ground states of spin glasses with high accuracy typically within $O(N^3)$ update steps, at least for system sizes up to $N \leqslant 256$ as studied here for the EA model. We read off and average the local fields for the presumed zero-temperature configuration found for each instance. For each reported system, between $10^4 - 10^5$ instances have been optimized, depending on system size. Since EO finds near-optima using a far-from-equilibrium dynamics, the explored configurations may possess a systematic bias. To check that this is not the case we have applied EO to reproduce $P(h)$ for the SK model (with $J_{ij} \in \{\pm N^{-1/2}\}$) for $N \leqslant 1023$,

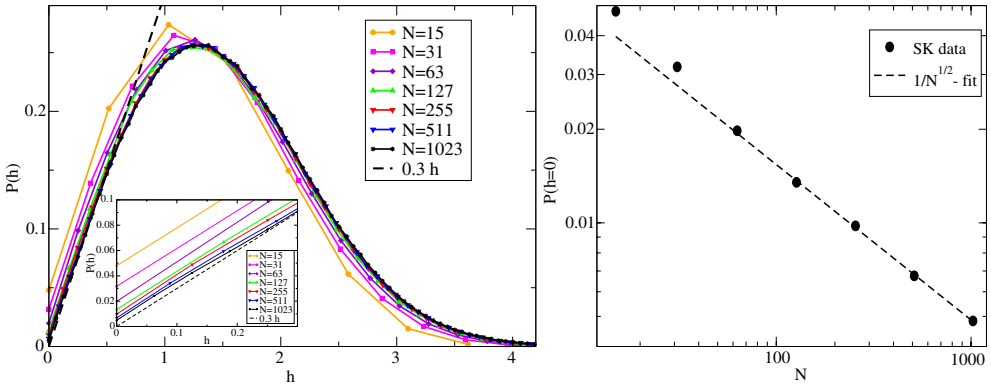

Figure 2. Left panel: $P(h)$ for $h \geqslant 0$ for SK systems of sizes $N = 15, \ldots, 1023$ at $T = 0$. (Here, a bimodal bond distribution, $J = \pm 1/\sqrt{N}$, has been used.) Clearly, the curves are well converged for the larger system sizes. The inset shows an enlargement of $P(h)$ for h near zero. The slopes are all ≈ 0.3, as indicated by the dashed line. Right panel: $P(h = 0) \sim 0.153(3)N^{-1/2}$, i.e., the data extrapolate to zero in the thermodynamic limit. The low noise in the data suggests that errors are smaller than the symbols.

as studied in [22], finding no such biases. This is apparent from figure 2, in which familiar properties (discussed below) of $P(h)$ in the SK model are reproduced, such as the linear slope for $|h| \to 0$ and the finite-size scaling of $P(h = 0) \sim 1/\sqrt{N}$ for $N \to \infty$.

For the KAS model, we use exchange (parallel tempering) Monte Carlo for the simulations [23]. To measure the local field distributions we compute 5000 disorder realizations for each system size N and value of σ. The lowest temperature simulated is $T = 0.05$ which is close enough to $T = 0$ such that for the system sizes studied we effectively probe the ground state of the system[4]. We also note that earlier studies of the SK model [8] have shown that $P(h = 0, T) = \lambda T + O(T^2)$ with $\lambda \approx (2\pi e)^{-1/2} \approx 0.25$, giving a deviation of ≈ 0.01 for the SK model at $T = 0.05$ compared with $T = 0$, which is indeed negligible compared to the values we find for small h for finite-range models.

In this study we consider $\sigma = 0.00$ (SK), 0.55 (MF), 0.75 (LR$^+$), 0.83 (LR$^+$), 1.00 ($\sigma = d$) as well as 1.50 (LR^0) and 2.00 (SR); see figure 1 for details. For all system sizes N and exponents σ we study $N_T = 29$ replicas. For $\sigma \leqslant 1.0$ we equilibrate the system for $N_{\rm sw} = 2^{17}$ Monte Carlo sweeps for $N \leqslant 128$ and for 2^{20} Monte Carlo sweeps for $N = 256$. For $1.50 \leqslant \sigma \leqslant 2.0$ we again take 2^{17} Monte Carlo sweeps to equilibrate for $N \leqslant 64$ but increase to 2^{19} Monte Carlo sweeps for $N = 128$. Then in each case we measure the local field distributions for the same amount of Monte Carlo time. Equilibration is tested by comparing the energy calculated from the link overlap to the internal energy of the system calculated directly. Once both agree, the system is considered to be in thermal equilibrium. For details see [20, 24].

4. Local field distributions

The local field distribution is defined by

$$P(h) = \left[\left\langle \frac{1}{N} \sum_i \delta \left(h - \sum_j J_{ij} S_j \right) \right\rangle \right]_{\rm av}, \tag{4}$$

[4] Tests have shown that for $N = 512$, 99% of the time the ground state of the system is probed (not shown—unpublished results). This number increases for decreasing system size. For example, for system sizes $N \leqslant 256$ all ground states of 10^4 trial samples were found.

where $\langle\cdots\rangle$ indicates a thermodynamic average and $[\cdots]_{\rm av}$ denotes an average over the quenched disorder.

The simplest nontrivial mean-field solution for $P(h)$ for the SK or EA models, the replica-symmetric [4, 11, 25] effective field approximation, yields $P(h)$ self-consistently through

$$P(h) = \frac{1}{\sqrt{2\pi q}}\, \mathrm{e}^{-h^2/2q}, \qquad q = \int \mathrm{d}h\, P(h) \tanh^2(\beta h), \tag{5}$$

where $\beta = 1/T$ is the inverse temperature. However, this approximation incorrectly yields a hole in $P(h)$ as $T \to 0$ [25], i.e., $P(h) = 0$ for all $|h| < (2/\pi)^{1/2}$.

Indeed, Thouless, Anderson and Palmer [3] argued already in 1977 that for small fields h in the SK model $P(h, T = 0) \sim 0.3|h|$, linearly in $|h|$.[5] Later studies of the SK model, employing full replica symmetry breaking (FRSB) [26], have borne out this linear form and the value of its slope (see, for example, figure 2 and [8, 10, 27]). Through accurate studies of a large sequence of finite-replica-symmetry breakings, references [9, 10] have demonstrated that within replica theory the correct linear behaviour of $P(h)$ for the SK model requires the full limit of infinite replica-symmetry breaking order; any finite-order truncation yielding a fictitious (if decreasing with RSB order) hole in $P(h)$ near $h = 0$.

Another model that is exactly solvable is the one-dimensional nearest-neighbour random-exchange Ising chain (limit of the KAS model for $\sigma \gg 1$), the one-dimensional EA model [8, 28]. It does not, however, have either frustration or a finite-temperature phase transition and, thus, no spin-glass phase. $P(h)$ is given by

$$P(h) = \int \mathrm{d}J \mathcal{P}(J)\mathcal{P}(h + J)\left\{1 - \tanh[\beta J]\tanh\left[\beta(h + J)\right]\right\}, \tag{6}$$

with

$$\mathcal{P}(J) = \frac{1}{\sqrt{\pi}}\, \mathrm{e}^{-J^2}, \tag{7}$$

such that $\langle J^2\rangle = 1/2$. For $\beta \to \infty$, this evaluates to

$$P(h) = \frac{2}{\pi}|h| \int_0^1 \mathrm{d}x\, \mathrm{e}^{-h^2(2x^2-2x+1)}, \tag{8}$$

again giving $P(h = 0) = 0$ and a linear small-h behaviour, analogously to the SK model, but with a slope almost twice as large, i.e., $P(h) \sim 2|h|/\pi$.

In higher dimensions the EA model is not exactly solvable. There is no finite-temperature spin-glass phase in $d = 2$, although there is such a phase [31] in $d = 3$ and greater. Yet, it is not clear that the glassy phase for $d \geqslant 3$ exhibits the characteristics of replica-symmetry breaking (e.g., ultrametricity) found in the SK model; at least up to an upper critical dimension believed to be $d_{\rm ucd} = 6$. We have performed a numerical simulation of $P(h)$ for the EA model using the EO heuristic [21]. The results are exhibited in figure 3. (Since $P(h)$ is symmetric, we only show plots for $h \geqslant 0$, i.e., $\int_0^\infty P(h)\,\mathrm{d}h = 1/2$.) At first sight $P(h)$ at $T = 0$ shows very little variation between the dimensions d; the overall shape is quite similar to that for the SK model, see figure 4. But, in fact, at closer detail there is a notable distinction for $h \to 0$, where the behaviour for the EA model differs significantly from the SK model. Unlike for the SK model (see figure 2), $P(h = 0)$ appears to be finite in the thermodynamic limit of the EA model, as the plot near $h = 0$ in the bottom panels of figure 3 indicate. We have extrapolated the values of $P(0)$ to infinite system size L in figure 5. For each $d \geqslant 2$, whether above or below the lower critical dimension, $P(0)$ quickly settles to a positive value between

[5] Actually, in [3] the authors give a bound on the coefficient but also express the belief that this bound should be saturated.

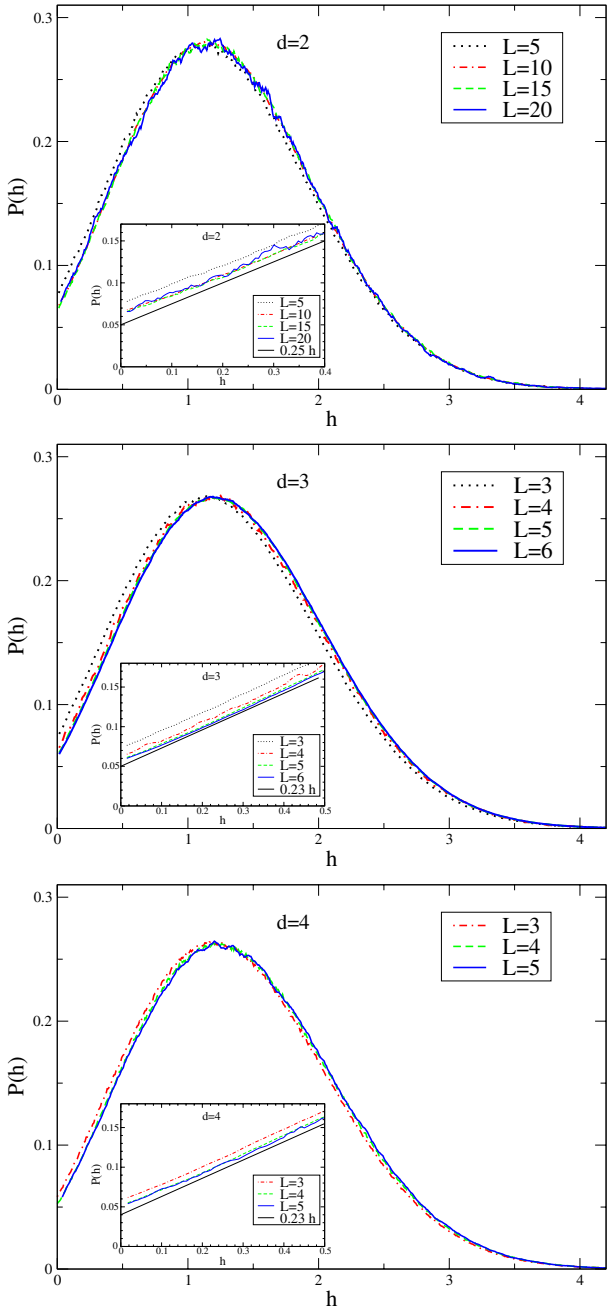

Figure 3. $P(h)$ for $h > 0$ for the EA spin glass on hyper-cubic lattices for $d = 2, 3$ and 4 for various side-lengths L for a Gaussian bond distribution with $\langle J^2 \rangle = 1/(2d)$. Already beyond some small L, there is little distinction between $P(h)$ for different sizes, indicating only small corrections to scaling. This becomes even more apparent in the insets, showing an enlargement of the data near $h = 0$. $P(h)$ in each d seems to converge to a finite value at $h = 0$ of $P(h = 0) \approx 0.065$ ($d = 2$), $P(h = 0) \approx 0.055$ ($d = 3$) and $P(h = 0) \approx 0.045$ ($d = 4$), see figure 5. $P(h)$ for small $|h|$ rises with a slope of $a \approx 0.25$ ($d = 2$), $a \approx 0.23$ ($d = 3$) and $a \approx 0.23$ ($d = 4$), where $P(h) \sim P(0) + a|h|$.

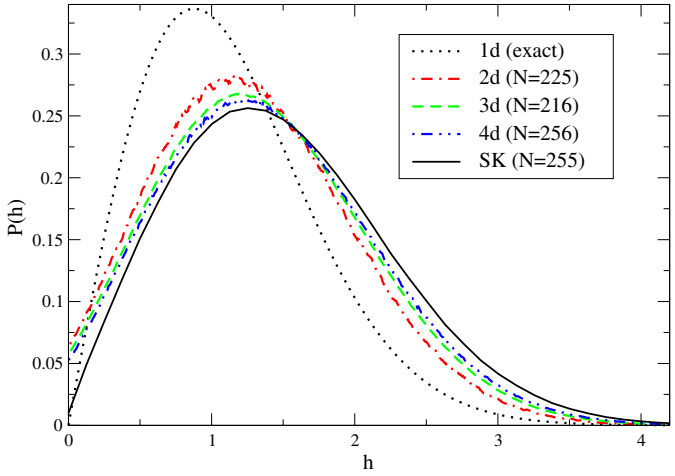

Figure 4. $P(h)$ for $h > 0$ for the EA spin glass in $d = 2, 3$ and 4 dimensions and for the SK model, all at comparable system size $N = 216, \ldots, 256$ for bond distributions with $\langle J^2 \rangle = 1/z$, where z is the connectivity of each spin: $z = 2d$ for the EA model and $z = N - 1$ for the SK model. Also plotted is the *exact* $d = 1$ result from equation (8). The plot highlights the overall similarity in $P(h)$ for all models and space dimensions. Except for $|h|$ close to zero, the numerical data for the EA model in $d = 2$–4 overall seem to interpolate monotonically between the $d = 1$ result and the SK ($d = \infty$) model. Yet, while $P(0) = 0$ for both $d = 1$ and SK, for $d = 2$–4, $P(0)$ is positive and monotonically decreasing, see figure 5.

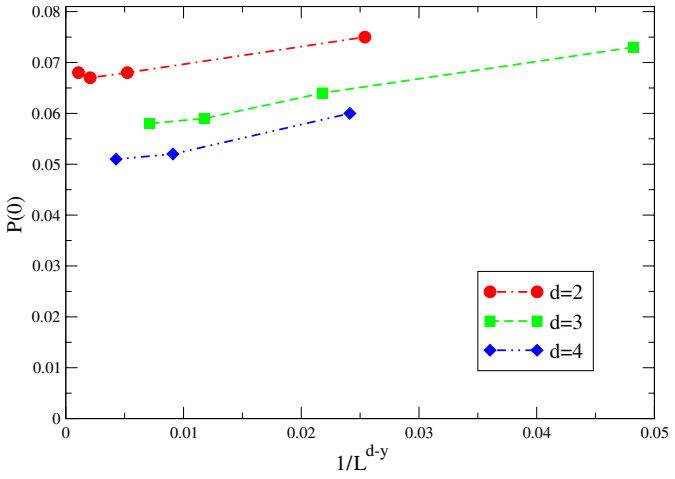

Figure 5. Extrapolation of the values for $P(0)$ obtained for $d = 2$, 3 and 4 in figure 3 for various system sizes L. The extrapolation to the thermodynamic limit $L \to \infty$ proceeds on a scale of $1/L^{d-y}$, where y for each d is the stiffness exponents discussed in [14]. As $P(h)$ has units of inverse energy, these are the appropriate corrections to scaling for the EA model [29, 30]. Clearly, $P(0) > 0$ for each d at $L \to \infty$, unlike for the SK model. The noise in the data suggests errors to be about double the size of the symbols.

approximately 0.04 and 0.07. This value seems to decrease slowly with increasing space dimension d, consistent with $P(0) = 0$ in the SK ($d = \infty$) limit; see figure 13. $P(h) - P(0)$ rises linearly for small h with a weakly d-dependent slope of $a \approx 0.23$–0.25.

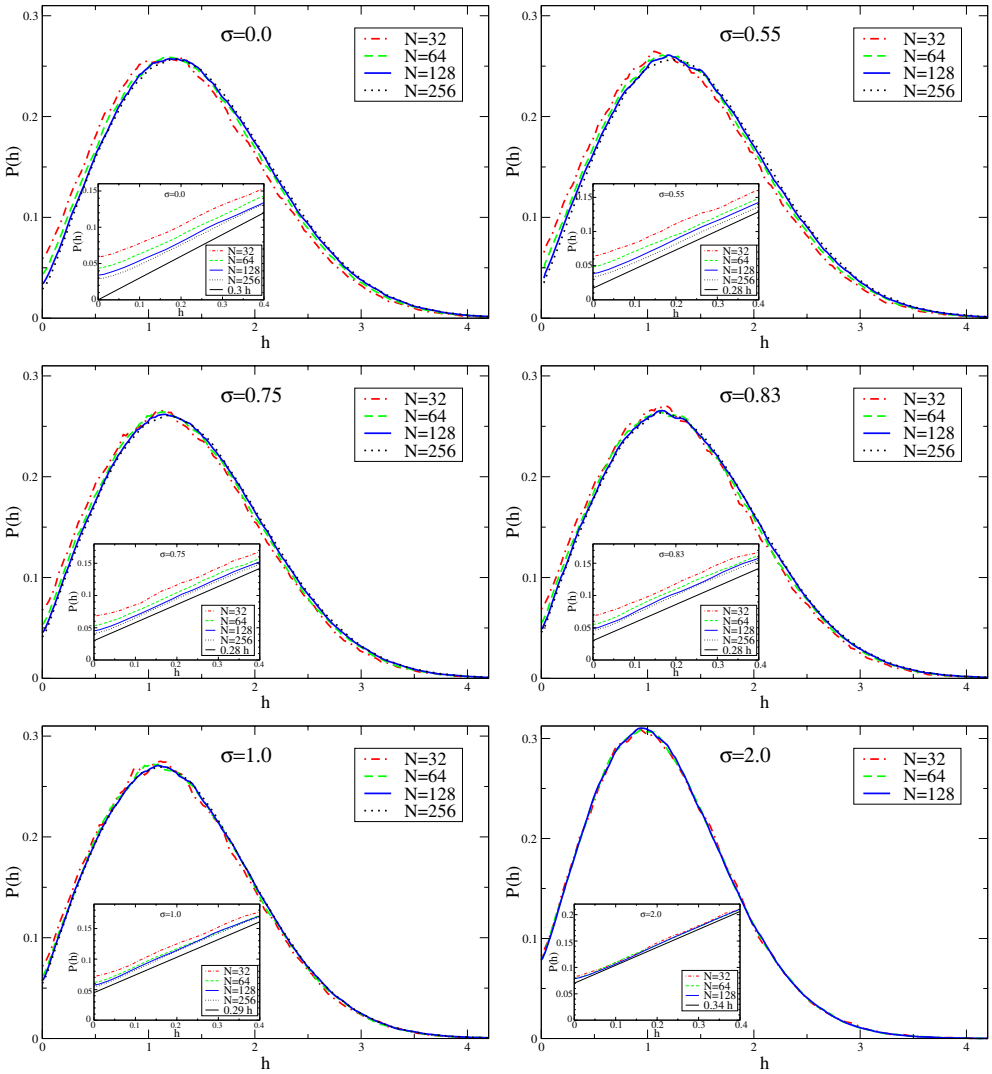

Figure 6. $P(h)$ for $h > 0$ and different system sizes N for the KAS model in $d = 1$ for different powers of the exponent σ which change the effective space dimension. The data are for the lowest temperature simulated, $T = 0.05$. The insets show an enlargement of the area around $h = 0$. $P(h = 0)$ clearly converges to a finite value for all $\sigma > 0.5$ and shows an approximately linear behaviour $[P(h) - P(0)] \sim 0.3|h|$ for small $|h|$. Note that the corrections to scaling decrease considerably for larger σ values.

We have performed a similar set of simulations for the $d = 1$ KAS model for a range of different σ values covering different behaviours ranging from SK-like to finite-range non-ordering ($T_c = 0$) [17]. In figure 6, we show the local field distributions for $T = 0.05$ for different system sizes N. Each panel is for a different exponent σ in equation (2). The similarity of all data sets for different σ is clearly visible. The insets show always the area around $h = 0$ in detail. To further illustrate the similarities between the data sets, in figure 7 we show data for $P(h)$ for $N = 128$ and different exponents σ covering all possible universality classes. The data for all σ agree relatively well, with the data for $\sigma > 1.0$ showing a more pronounced

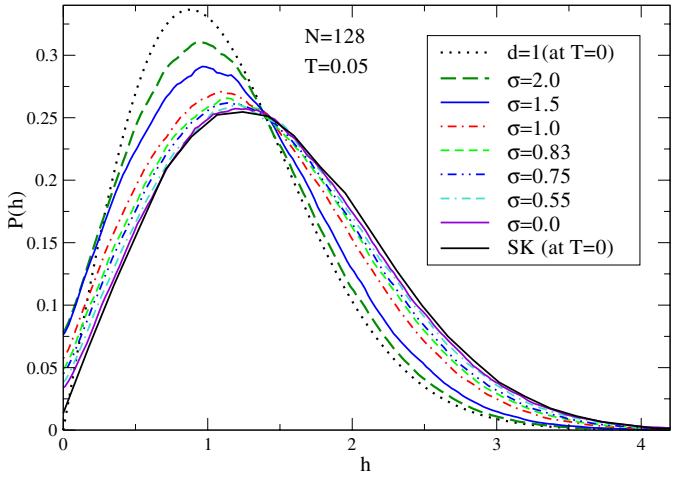

Figure 7. Direct comparison of the local field distribution $P(h)$ (at $T = 0.05$) as a function of the local field h for the KAS model and $N = 128$ spins and different values of the exponent σ covering all possible universality classes from infinite range to short range with zero transition temperature. Also plotted are the exact results for $d = 1$ (i.e., $\sigma \to \infty$) from equation (8) and the SK data (i.e., $\sigma = 0$) from figure 2 (both at $T = 0$). As in figure 4, the data interpolate smoothly between both extremes, except at $P(0)$.

peak and larger gap. Again, for the different values of $\sigma > 0.5$ studied, $[P(h) - P(0)] \sim a|h|$ for $|h|$ small with $a \approx 0.3$ interpolating between the SK and the short-range one-dimensional result[6].

We have also extrapolated the data for $P(h = 0, T, N)$ to $T = 0$ (fits to a quadratic function for $T \leqslant 0.3$ with fitting probabilities [32] larger than ~ 0.3). A typical example of the extrapolation for $\sigma = 0.83$ is shown in figure 8 (the behaviour of $P(h)$ for different temperatures is shown in figure 9). Since the difference between $T = 0.05$ and $T = 0$ is minimal and because estimating the error bars for the extrapolated data is difficult, in figure 10 we show data for $T = 0.05$.

A closer look at figures 7 and 10 poses an interesting question: in the KAS model, $P(0)$ appears to be an increasing function of σ for all values studied so far, rising from $P(0) = 0$ at $\sigma = 0$ for SK to $P(0) \approx 0.08$ at $\sigma = 2.0$. Yet, the exact result for the one-dimensional Ising chain, corresponding to $\sigma = \infty$, again has $P(0) = 0$. Hence either the apparent extrapolation to the limit $N \to \infty$ limit, shown in figure 10, is incorrect and $P(0) = 0$ for all σ after all, or there has to be a maximum in $P(0)$ at some finite $\sigma_{\max}$ beyond which $P(0)$ again descends to zero. To decide this question, we have done a more extended study of $P(0)$ also for $\sigma > 2.0$ which is shown in figure 11. The results clearly show a well-defined maximum near $\sigma_{\max} \approx 1.8$, which is likely to persist in the thermodynamic limit. The resolution of this question—surprising in its own right—strengthens our belief that finite-size effects in our presentation are well under control. In all, the KAS model essentially reproduces the results found for the SK and canonical EA models for $\sigma \lesssim 1$, where it corresponds to possible physical dimensions and for larger σ (where the formula $d_{\text{eff}} \approx 2/(2\sigma - 1)$ [13] becomes inappropriate) it continues smoothly towards the nearest-neighbour $d = 1$ EA limit. The fact that $P(0)$ peaks for the KAS model at a value of σ intermediate between that corresponding to

[6] It has been shown [38] that system sizes of $N \gtrsim 200$ are needed to probe the thermodynamic limit of the KAS and SK models. The local field distributions $P(h)$ show small corrections to scaling and thus the system sizes studied in this work should suffice.

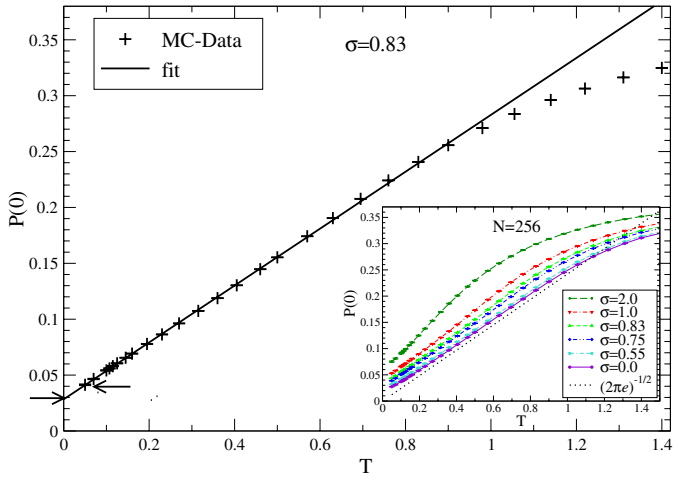

Figure 8. $P(h = 0)$ as a function of temperature for $\sigma = 0.83$ and $N = 256$. The data are well fit by a linear behaviour in T (with very small quadratic corrections) with slope ≈ 0.25 for $T \leqslant 0.3$. Data for $T = 0.05$ are very close to $T = 0$ (arrows), which is why in figure 10 we extrapolate to $N = \infty$ for $T = 0.05$ and not $T = 0$. Furthermore, the estimate of the error bars in the temperature extrapolation is difficult. Inset: $P(h = 0)$ for a range of σ compared with the SK result $(2\pi \mathrm{e})^{-1/2}T$.

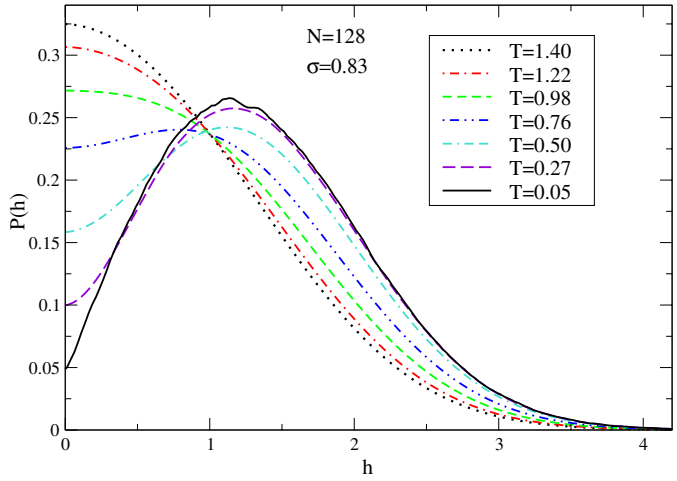

Figure 9. $P(h)$ for $\sigma = 0.83$ and $N = 128$ for different temperatures ranging from $T = 0.05$ to temperatures well above the transition temperature T_c. For low enough T the local field distribution shows a dip around $h = 0$ which is 'filled in' for increasing temperatures. For $T \gg T_c$ we obtain a Gaussian distribution.

$d_{\mathrm{eff}} = 2$ and $d_{\mathrm{eff}} = 1$ suggests that if one could continue the EA model off integer dimensions, there might exist a dimension $d_{\max}$, likely between $d = 1$ and $d = 2$ at which $P(0)$ would peak. The slope of $[P(h) - P(0)]$ near $h = 0$ is however found to vary monotonically with σ between the SK ($\sigma = 0$) and nearest-neighbour EA ($\sigma = \infty$) limits.

The local field distribution $P(h)$ for a disordered Ising spin system with Gaussian distributed random exchange disorder is thus seen to be remarkably robustly linear in $|h|$ at low h with a coefficient in the range $a = 0.25$–0.35, irrespective of whether the system exhibits

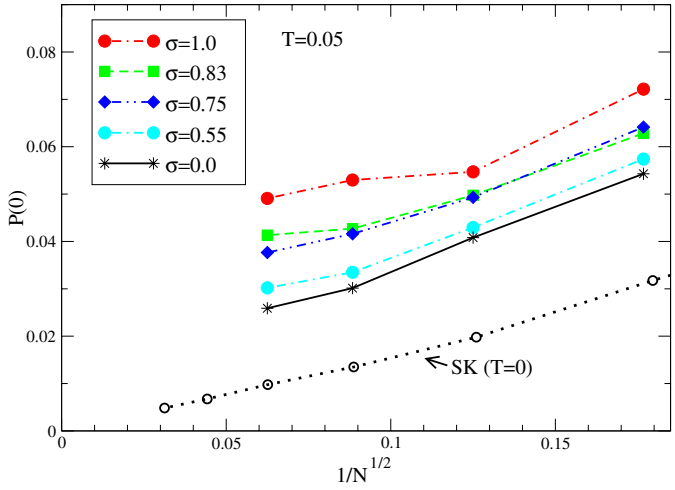

Figure 10. Extrapolation of the values for $P(0)$ obtained for the KAS model as a function of $1/\sqrt{N}$ for $T = 0.05$ and different values of the exponent σ. The data for $\sigma = 0.00$ decay with a power-law similar to the SK model. For larger values of σ the data indicate a saturation to a finite value of $P(0)$ for $N \to \infty$. Larger system sizes would be needed to clearly differentiate the different scenarios beyond a qualitative comparison. The noise in the data suggests an error of about five times the symbol size. For comparison we also show the data for SK at $T = 0$ from figure 2; note that the shift compared with the $\sigma = 0$ KAS results is due to the finite-temperature shift $(2\pi e)^{-1/2}T$.

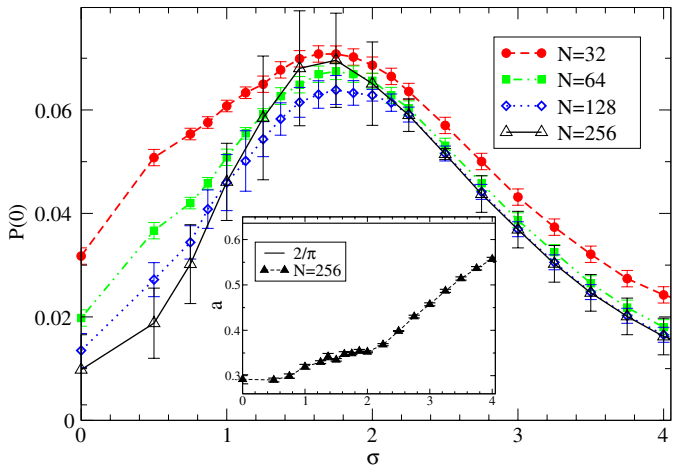

Figure 11. Plot of $P(0)$ as a function of σ in the KAS model. For each data point in $N = 32$ and 64 averaged $P(h)$ over at least 10^5 instances, 210^4 instances at $N = 128$, and at least 10^3 for $N = 256$. (The data for $N = 256$ clearly show a systematic bias *only* near the maximum, indicative that those instances are hardest to optimize. Note the complete lack of residual finite size effects for $\sigma > 2.0$.) To obtain smooth estimates of $P(0)$, independent of the width of histograms chosen to measure $P(h)$, we made a linear fit to the respective $P(h)$ for $h < 0.3$ to obtain each data point. Inset: Plot of the slope $a = \partial P(h)/\partial h|_{h\to 0}$ of $P(h)$ near $h = 0$ as a function of σ, extracted from a fit to the same data. Only data for $N = 256$ are shown, as there are hardly any finite size effects. $2/\pi$ (solid line) represents the slope for the one-dimensional result in equation (8) obtained for $\sigma \to \infty$.

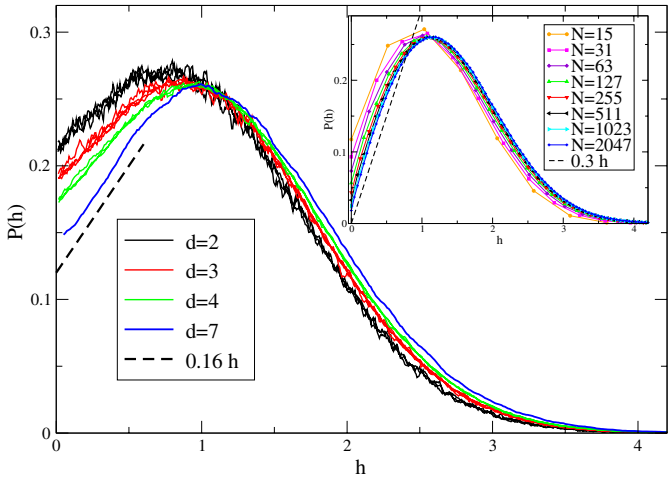

Figure 12. Local field distribution $P(h)$ for the EA model in $d = 2$, 3 and 4, obtained after purely relaxational single-spin dynamics on 10^4 instances for each L and d. The same system sizes L as in figure 3 have been used here but finite-size effects are well below the statistical noise. We have added results for $d = 7$ ($L = 3$) to show that there are no drastic changes above the upper critical dimension $d_{\rm ucd} = 6$. The dashed line merely serves to guide the eye. Inset: $P(h)$ for relaxational single-spin dynamics in SK.

spin-glass order and independent of whether such spin-glass order is replica-symmetry-broken mean field or not.

It is also interesting to compare with studies of a non-equilibrated SK model [33–35]. In these studies, spins are initially randomized and then exposed to purely relaxational single-spin dynamics, i.e., dynamics in which spins are chosen randomly and flipped if and only if such a flip would reduce the energy, until a metastable state is reached. The distribution $P(h)$ averaged over only those metastable states reached by this procedure is again linear in $|h|$ for small h with a slope that again appears to be of order $a \sim 0.3$. The interest of this observation in the present context is that the metastable states reached in this dynamical procedure are not the ground state. Indeed they are significantly above the ground state, with the average relaxational energy variously reported as $E_{\rm relax}/N \approx -0.7$ [34], -0.715 [33] and -0.73 [35], much higher than the ground-state energy per spin $E_{\rm gs}/N = -0.7632$ [10], while the corresponding $P(h, E_{\rm relax})$ averaged over all metastable states has a finite value at $h = 0$ [33, 34].

We have conducted a comparable study of $P(h)$ over metastable states reached by rapid quench for the EA model in $d = 2, 3, 4$ and 7, and SK, as shown in figure 12. As for the results for the SK model, there are significant (qualitative) similarities between the $T = 0$ equilibrium results of $P(h)$ in figure 3 and those obtained by simple relaxation. But especially the behaviour near $h = 0$ deviates quantitatively, with $P(0)$ distinctly larger and the initial slope significantly smaller. Yet, both seem to tend smoothly towards the corresponding SK result $P(0) = 0$ (see figure 2 and [33, 34], respectively) for $d \to \infty$, as is demonstrated in figure 13. Furthermore, for small $|h|$ the local field distribution shows a linear behaviour as found in [36] via an intrinsically far-from-equilibrium simulation along the hysteresis loop of the model for finite external fields. Finally, as in [33, 34], the metastable states obtained under relaxation in the EA model are substantially more energetic than the ground states. For instance, in $d = 3$ relaxation gives a normal distribution of states of mean $E_{\rm relax}/N \approx -1.4$ and a deviation of approximately 0.1, whereas the ground states found at $L = 6$ are centred

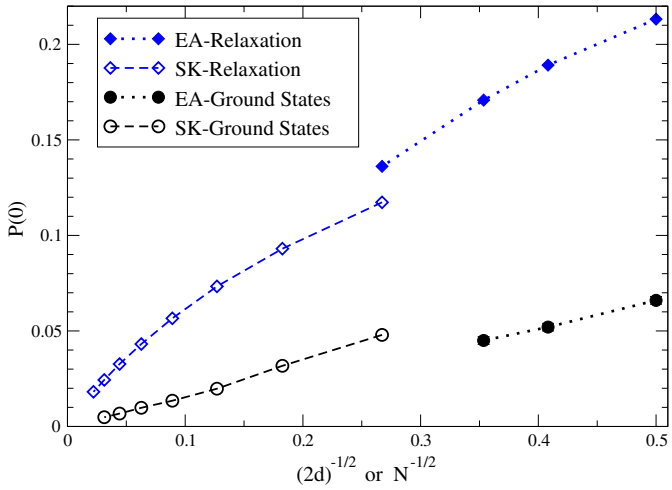

Figure 13. Extrapolation of $P(0)$ towards the SK-limit, $d \to \infty$. Shown are the values of $P(0)$ obtained from the $L \to \infty$ extrapolation in figure 5 for ground states of the EA model (full circles) and those obtained by a relaxation process of the data shown in figure 12 (full diamonds), which are approximately L-independent. Added are the data points for SK for ground states from figure 2 (open circles) and for relaxation from figure 12 (open diamonds). As the EA spin glass approaches the SK model by setting $2d = N - 1 \to \infty$, the appropriate scale here is $(2d)^{-1/2} \sim N^{-1/2}$, according to the right panel of figure 2. Asymptotic slopes for the SK data are 0.153(3) for ground states and approximately 0.61 for relaxation (see also [35]). For both sets of data, it seems that $\lim_{d\to\infty} P(0) \to 0$, consistent with the respective SK results. Similar to the case of $\sigma > 0.5$ in figure 11, there is no indication here that $P(0) = 0$ for any $d < \infty$.

just above $E_{\rm gs}/N \approx -1.7$, with a much narrower deviation and close to the thermodynamic value of $-1.700(1)$. [37]

Finally in this section, let us return to figure 8 now concentrating on the gross T-dependence. This figure demonstrates another robust feature, the linearity of $P(h = 0, T)$ with T up to the mean-field transition temperature $T_{\rm MF} = 1$; this result previously observed in the SK model [8] is seen from the main figure to hold well also for the KAS model with $\sigma = 0.83$, even though the actual transition temperature in this case is much smaller than the mean-field temperature (indeed it is closer to $T_{\rm c} = 0.45$ [20]). As shown in the inset, a similar behaviour is found for other values of σ (up to the order of the peak in figure 11), the higher of which have no finite-temperature phase transition. Thus again the general shape of $P(h = 0, T) - P(h = 0, T = 0)$ is rather robust against whether the system is one which orders or not, has RSB or not.

5. Conclusions

We have presented results for the local field distributions of different spin-glass models in different space dimensions. These include both cases where there is generally believed to be a finite-temperature phase transition and others where no finite temperature transition occurs. They also include cases where the subtleties of replica symmetry breaking are believed to operate and others where they do not occur or are in question. Our results show that the distributions of local field are qualitatively very similar for all models with Gaussian-distributed interactions; the data for $P(|h|, T = 0)$ decay exponentially for large fields $|h|$ and show a linear behaviour for $|h|$ close to zero. The distributions only show differences in behaviour near

$T = 0$ and $h = 0$ where for the infinite-range SK model $P(h = 0, T = 0, N) \sim N^{-1/2} \to 0$ as $N \to \infty$, while all other finite-dimensional Edwards–Anderson spin-glass models studied with space dimensions $d > 1 P(h = 0, N)$ seem to tend to a constant in the thermodynamic limit. For finite d the thermodynamic value of $P(0)$ scales as $d^{-1/2}$ for low d with a coefficient very close to that for the SK model, taking $2d = N - 1$ to match coordination number for spins in EA and SK, see figure 13. This suggests that $d^{-1/2}$-scaling applies for all d.[7]

These observations are mirrored by simulations of a one-dimensional Ising model with random power-law interactions: for the regime of the power-law exponent σ which correspond to an infinite-ranged system, $P(h = 0)$ decays with an inverse power of the system size, whereas for all other universality classes the distributions tend to a constant in the thermodynamic limit, rising from zero in the limits of both SK $\sigma = 0$ and the unfrustrated nearest-neighbour $\sigma = \infty$, with a maximum for σ near 2. Furthermore, for all σ the $P(h = 0, T)$ are all close to the same linear-T behaviour for $T < T_{\mathrm{MF}} = 1$.

Qualitatively similar, but quantitatively different, small-h $P(h)$ behaviour is also found for systems that are quenched from random starts (to states that are not thermodynamically equilibrated).

Our study has been concerned with the case of Gaussian exchange distribution. For problems with discrete distributions, such as for J_{ij} randomly $\pm J$ one expects $P(h = 0, T = 0)$ to be nonzero for finite-range systems [8]. It is, however, surprising how small the observed $P(h = 0, T = 0)$ are for Gaussian exchange disorder without being zero. This effectively counsels against associating small $P(0)$ and simple small-h slopes with the subtleties of RSB or finite-temperature spin-glass transitions[8].

Finally, we should caution that the simulations were performed for finite system sizes and although corrections to scaling seem to be very small, a change in behaviour at larger system sizes cannot be ruled out completely.

Acknowledgments

We would like to thank H Horner, M Müller and G T Zimanyi for helpful comments and suggestions. SB acknowledges support from the Division of Materials Research at the National Science Foundation under grant no 0312510 and from the Emory University Research Council. HGK acknowledges support from the Swiss National Science Foundation under grant no PP002-114713. Part of the simulations were performed on the Hreidar and Gonzales clusters at ETH Zürich. DS acknowledges support from the UK Engineering and Physical Sciences Research Council under grant no D050952.

References

[1] Marshall W 1960 *Phys. Rev.* **118** 1519
[2] Klein M W and Brout R 1963 *Phys. Rev.* **132** 2412
[3] Thouless D J, Anderson P W and Palmer R G 1977 *Phil. Mag.* **35** 593
[4] Sherrington D and Kirkpatrick S 1975 *Phys. Rev. Lett.* **35** 1792
[5] Mézard M, Parisi G and Virasoro M A 1987 *Spin Glass Theory and Beyond* (Singapore: World Scientific)
[6] Talagrand M 2003 *Spin glasses: a Challenge for Mathematicians* (Berlin: Springer)
[7] Palmer R G and Pond C M 1979 *J. Phys. F: Met. Phys.* **9** 1451
[8] Thomsen M, Thorpe M F, Choy T C, Sherrington D and Sommers H J 1986 *Phys. Rev.* B **33** 1931
[9] Oppermann R and Sherrington D 2005 *Phys. Rev. Lett.* **95** 197203

[7] We are grateful to M Mueller for drawing our attention to this correspondence.
[8] A corollary is to anticipate in disordered semiconductors similar lack of connection between a 'Coulomb gap' in the density of states centred at the Fermi level [39] and the existence or otherwise of a glassy state [40, 41].

[10] Oppermann R, Schmidt M J and Sherrington D 2007 *Phys. Rev. Lett.* **98** 127201
[11] Edwards S F and Anderson P W 1975 *J. Phys. F: Met. Phys.* **5** 965
[12] Sherrington D and Southern B W 1975 *J. Phys. F: Met. Phys.* **5** L49
[13] Binder K and Young A P 1986 *Rev. Mod. Phys.* **58** 801
[14] Boettcher S 2005 *Phys. Rev. Lett.* **95** 197205
[15] Fisher D S and Huse D A 1988 *Phys. Rev.* B **38** 386
[16] Kotliar G, Anderson P W and Stein D L 1983 *Phys. Rev.* B **27** R602
[17] Katzgraber H G and Young A P 2003 *Phys. Rev.* B **67** 134410
[18] Katzgraber H G and Young A P 2003 *Phys. Rev.* B **68** 224408
[19] Katzgraber H G, Körner M, Liers F, Jünger M and Hartmann A K 2005 *Phys. Rev.* B **72** 094421
[20] Katzgraber H G and Young A P 2005 *Phys. Rev.* B **72** 184416
[21] Boettcher S and Percus A G 2001 *Phys. Rev. Lett.* **86** 5211
[22] Boettcher S 2005 *E. Phys. J.* B **44** 317
[23] Hukushima K and Nemoto K 1996 *J. Phys. Soc. Japan* **65** 1604
[24] Katzgraber H G, Palassini M and Young A P 2001 *Phys. Rev.* B **63** 184422
[25] Schowalter L J and Klein M W 1979 *J. Phys. C: Solid State Phys.* **12** L935
[26] Parisi G 1980 *J. Phys. A: Math. Gen.* **13** L115
[27] Pankov S 2006 *Phys. Rev. Lett.* **96** 197204
[28] Barma M and Sharma K C 1979 *Solid State Commun.* **30** 11
[29] Boettcher S 2008 Corrections to scaling in lattice spin glasses (unpublished)
[30] Campbell I A, Hartmann A K and Katzgraber H G 2004 *Phys. Rev.* B **70** 054429
[31] Katzgraber H G, Körner M and Young A P 2006 *Phys. Rev.* B **73** 224432
[32] Press W H, Teukolsky S A, Vetterling W T and Flannery B P 1995 *Numerical Recipes in C* (Cambridge: Cambridge University Press)
[33] Parisi G 1995 *Fractals (Supplementary Issue)* **11** 161 (*Preprint* cond-mat/9501045)
[34] Eastham P R, Blythe R A, Bray A J and Moore M A 2006 *Phys. Rev.* B **74** 020406
[35] Horner H 2007 *Eur. Phys. J.* B **60** 413
[36] Pázmándi F, Zaránd G and Zimányi G T 1999 *Phys. Rev. Lett.* **83** 1034
[37] Pal K F 1996 *Physica* A **233** 60
[38] Billoire A 2007 Some aspects of infinite range models of spin glasses: theory and numerical simulations *Preprint* cond-mat/0709.1552
[39] Efros A L and Shklovskii B I 1975 *J. Phys. C: Solid State Phys.* **8** L49
[40] Müller M and Ioffe L B 2004 *Phys. Rev. Lett.* **93** 256403
[41] Müller M and Pankov S 2007 *Phys. Rev.* B **75** 144201